

Weekly Report – W6 Fall 2022

Problem & Task

1. Book Reading

- (1). Biomechanics and motor control of human, Chapter 4 Anthropometry;
- (2). Neuromechanics of human movement;
- (3). A Mathematical Introduction to Robotic Manipulation, Chapter 2 Rigid Body Motion.

2. Paper Reading

- (1). About soft robotics PDE – energy shaping

3. Simulation

- (1). Single arm with free motion (no ball)
- (2). Single arm attached with a falling ball

4. Exoskeleton Optimization

- (1). Adhere foam on exoskeleton test equipment to avoid direct contact with subject's skin.

Solution & Summary

1. Book Reading

- (1). Human falling down motion modelling:

The motion of human falling down can be illustrated by a simplified model with variable of inclination angle (predefined) of the human, which was showcased in last week's report, however, the authentic case of fall can be much more complicated, for instance, the falling direction could be lateral and when human begins to fall forward, the morphological characteristic of human body could not be the same as a rigid bar, the lower limbs will take some actions autonomously to prevent this process. Given this situation, the human body can be modelled by multi-links with mass concentrated in the geometry center of each link, since the length, mass and inertia tensor of each link can be derived from experience and big data analysis as shown in the table below.

Segment	Definition	Segment Weight/Total Body Weight	Center of Mass/ Segment Length		Radius of Gyration/ Segment Length			Density
			Proximal	Distal	C of G	Proximal	Distal	
Hand	Wrist axis/knuckle II middle finger	0.006 M	0.506	0.494 P	0.297	0.587	0.577 M	1.16
Forearm	Elbow axis/ulnar styloid	0.016 M	0.430	0.570 P	0.303	0.526	0.647 M	1.13
Upper arm	Glenohumeral axis/elbow axis	0.028 M	0.436	0.564 P	0.322	0.542	0.645 M	1.07
Forearm and hand	Elbow axis/ulnar styloid	0.022 M	0.682	0.318 P	0.468	0.827	0.565 P	1.14
Total arm	Glenohumeral joint/ulnar styloid	0.050 M	0.530	0.470 P	0.368	0.645	0.596 P	1.11
Foot	Lateral malleolus/head metatarsal II	0.0145 M	0.50	0.50 P	0.475	0.690	0.690 P	1.10
Leg	Femoral condyles/medial malleolus	0.0465 M	0.433	0.567 P	0.302	0.528	0.643 M	1.09
Thigh	Greater trochanter/femoral condyles	0.100 M	0.433	0.567 P	0.323	0.540	0.653 M	1.05
Foot and leg	Femoral condyles/medial malleolus	0.061 M	0.606	0.394 P	0.416	0.735	0.572 P	1.09
Total leg	Greater trochanter/medial malleolus	0.161 M	0.447	0.553 P	0.326	0.560	0.650 P	1.06
Head and neck	C7–T1 and 1st rib/ear canal	0.081 M	1.000	— PC	0.495	0.116	— PC	1.11
Shoulder mass	Sternoclavicular joint/glenohumeral axis	—	0.712	0.288	—	—	—	1.04
Thorax	C7–T1/T12–L1 and diaphragm*	0.216 PC	0.82	0.18	—	—	—	0.92
Abdomen	T12–L1/L4–L5*	0.139 LC	0.44	0.56	—	—	—	—
Pelvis	L4–L5/greater trochanter*	0.142 LC	0.105	0.895	—	—	—	—
Thorax and abdomen	C7–T1/L4–L5*	0.355 LC	0.63	0.37	—	—	—	—
Abdomen and pelvis	T12–L1/greater trochanter*	0.281 PC	0.27	0.73	—	—	—	1.01
Trunk	Greater trochanter/glenohumeral joint*	0.497 M	0.50	0.50	—	—	—	1.03
Trunk head neck	Greater trochanter/glenohumeral joint*	0.578 MC	0.66	0.34 P	0.503	0.830	0.607 M	—
Head, arms, and trunk (HAT)	Greater trochanter/glenohumeral joint*	0.678 MC	0.626	0.374 PC	0.496	0.798	0.621 PC	—
HAT	Greater trochanter/mid rib	0.678	1.142	—	0.903	1.456	—	—

Table. W6-1 Anthropometric data of human body [1]

Based on the information above, to model the human motion, an example of simplified 3-

link model has been introduced in Fig. W6-1 with mass m_1 (legs and feet), m_2 (thighs, pelvis and trunk 1) and m_3 (upper limbs composed of head, trunk 2, 3, 4 and both upper and lower arms) by measuring the angles defined, the COM of each part can be determined so that the total equivalent COM of the whole body can be estimated by the equation below:

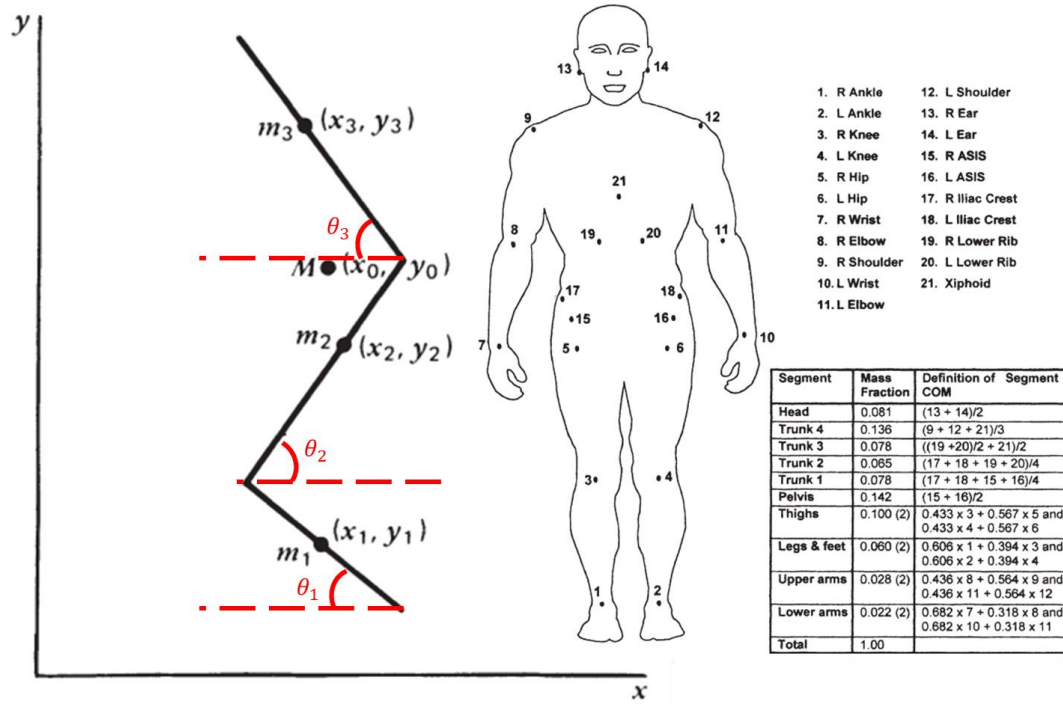


Fig. W6-1 The schematic of a 3-link human model and its mass fraction

$$x_0 = \frac{m_1 x_1 + m_2 x_2 + m_3 x_3}{m_1 + m_2 + m_3} = \frac{f_1 M x_1 + f_2 M x_2 + f_3 M x_3}{M} = f_1 x_1 + f_2 x_2 + f_3 x_3 \quad (W6 - 1)$$

where M is the total mass of body, f_1 , f_2 and f_3 stand for the mass fraction coefficients of each part respect to the whole body. And y_0 can be worked out in the same way.

Subsequently, the total COM position change can be converted into inclination angle change, which can be utilized to estimated the human's generalized force.

2. Simulation

(1). Supplement Assumptions

- The COM (center of mass) of each SRA segment (in arc shape) is deemed to be at the geometry center of the generalized chord. The proof is shown as follows.

According to the definition of COM of an arc shape, we have the distance between its COM and the center of complete circle below,

$$L_{OG} = \frac{2r}{\theta} \sin \frac{\theta}{2} \quad (W6 - 2)$$

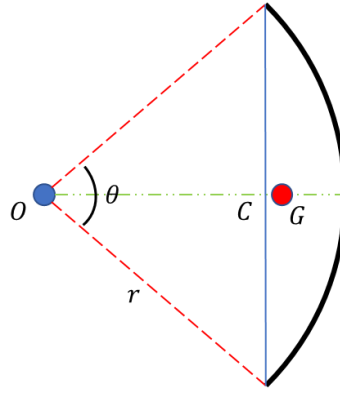


Fig. W6-2 The schematic of variable definition of an arbitrary arc

where point G is the COM of the arc and point C is the geometry center of the generalized chord, r is the curvature radius. The length of OC should be $L_{OC} = r \cos \frac{\theta}{2}$, $r = \frac{L}{\theta}$.

Thus the gap between point C and G will be

$$\Delta L = L_{OG} - L_{OC} = \frac{2r}{\theta} \sin \frac{\theta}{2} - r \cos \frac{\theta}{2} = r \left(\frac{2}{\theta} \sin \frac{\theta}{2} - \cos \frac{\theta}{2} \right) = \frac{L}{\theta} \left(\frac{2}{\theta} \sin \frac{\theta}{2} - \cos \frac{\theta}{2} \right) \quad (W6-3)$$

Two groups of control tests were performed based on the variation of bending angle ($35^\circ \sim 90^\circ$) and length ($0.1 \text{ m} \sim 1 \text{ m}$) of SRA segment, the results showed that the length of SRA domains the distance between COM of SRA and center of SRA chord, further influences the accuracy of the model.

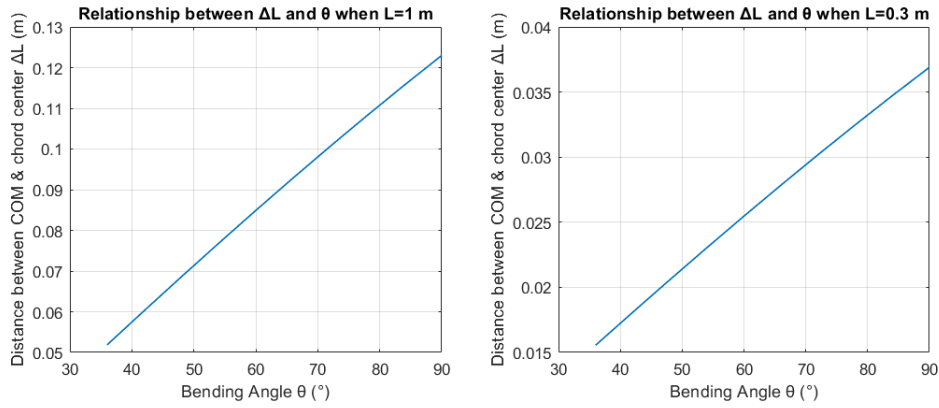


Fig. W6-3 Relationship between ΔL & L when $L = 1 \text{ m}$ and 0.3 m respectively

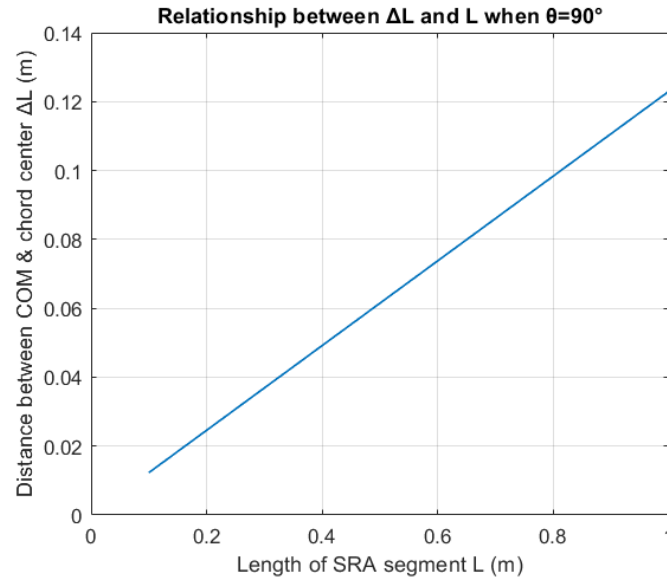


Fig. W6-4 Relationship between ΔL & L when $\theta = 90^\circ$

To evaluate this approach of simplified modelling, the length of each segment of SRA in our project has been measured, approximately 0.3 m as shown in the figure below, and the simulation results aforementioned showcased that even for large bending angle (90°), the magnitude of ΔL is very small, the authentic inertia tensor (adding this part by using inertial parallel theory) would not differ such a lot from that of the simulation model, which indicates that **the current model is reliable depending on the length of SRA**. In the future, if we plan to study the dynamics of longer SRA, we can divide each segment by multiple equal length cylinder bars (RPR manipulator) to improve its accuracy.



Fig. W6-5 Measured length of each SRA segment

- The two segments are continuous about the joint;

(2). Basic structure

Reference was taken from Chase's model, which will ease the coding work a lot, I have already defined the inertia, Corolis, damping, stiffness and gravitational matrices inside the "Model Dynamics" block in the figure below. Now I'm stuck by handling symbolic variable array partial differentiation, I will fix it as soon as possible, please give me some time.

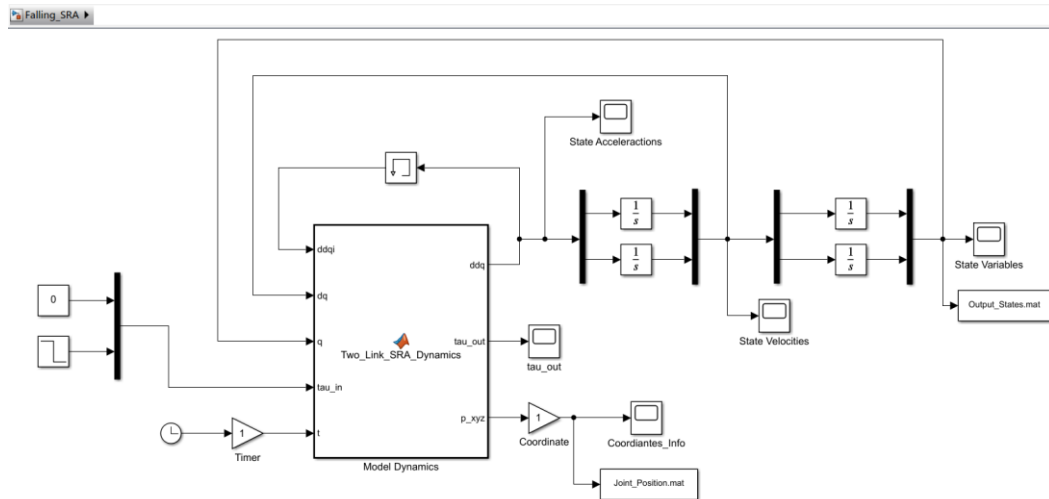


Fig. W6-6 The basic layout of the SRA Simulink model

3. Exoskeleton Optimization

As it will take several days for order shipping (the sticker foam), I adhered some trimmed foam on the exoskeleton test equipment, which is sort of rough, but it's just in alpha stage; meanwhile, I have already found some potential foam sheets via Buyways (in Excel), which will be more pro, please take it look. Afterwards, I will use them for our spare parts.

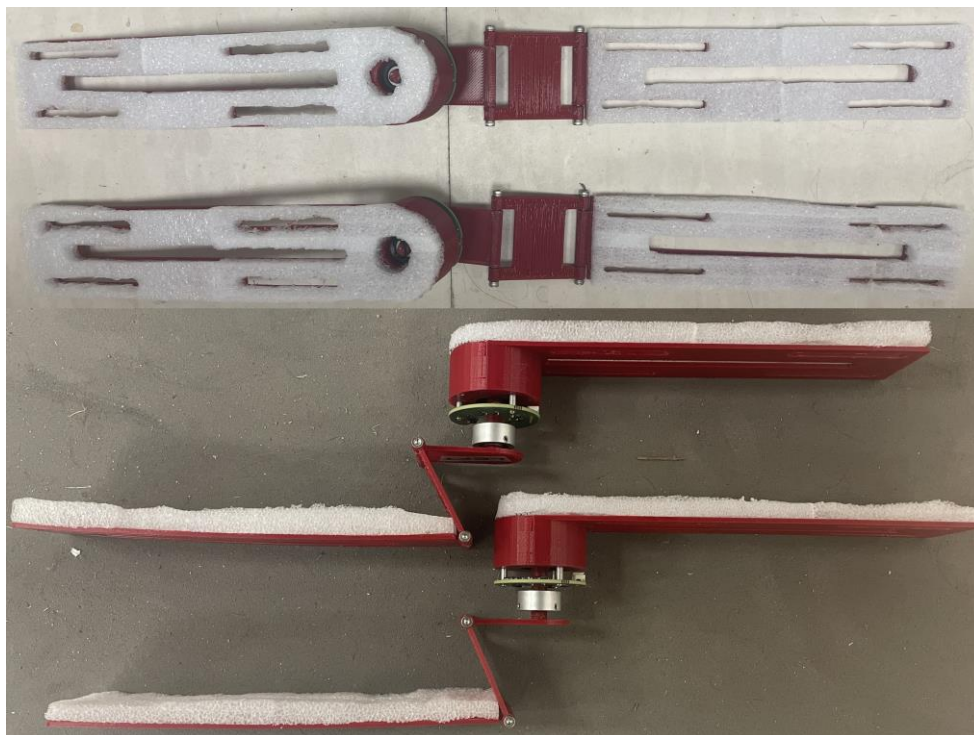


Fig. W6-7

Difficulty

1. About simulation: at the first stage, I was trying to use a more general way to derive the governing equation by symbolic variable in MATLAB, but there are some issues with the partial differentiation, I will figure it out very soon; on the other hand, I can use the manually derived version to assess the correctness of the dynamics, nevertheless, it's

unrealistic to derive the motion equation by hand every time, especially for more and more complicated scenarios in the future.

Plan

1. Finish reading the rest materials, no matter for books or papers;
2. Finish the simulation, if the partial differentiation works for symbolic variable array (for example, in our model, we have multiple angles $\theta(1), \theta(2)$), the Jacobian matrix can be successfully derived, it will not be a big deal for adding a ball at the end-effector of the SRA.

Reference

[1] Winter, D.A., 2009. *Biomechanics and motor control of human movement* John Wiley & Sons.